Dynamics of phase separation in copolymer-homopolymer mixtures

Takao Ohta and Aya Ito
Department of Physics, Ochanomizu University, Tokyo 112, Japan
(Received 15 March 1995)

We carry out computer simulations of phase separation in diblock copolymer-homopolymer mixtures. The homopolymer chains are assumed to be compatible with one of the blocks of the copolymers whereas the two blocks of the copolymer chains are mutually incompatible. One of the characteristic features of this system is that, in certain conditions, it undergoes a double phase separation. That is, by decreasing the temperature, a macrophase separation takes place so that copolymer-rich and homopolymer-rich domains are formed. As the phase separation proceeds, a microphase separation also starts in the copolymer-rich domains. We study the kinetics of this double phase separation and the domain morphology associated with the phase separations in two dimensions. It is shown that a morphological transition occurs by changing the incompatibility strength between the homopolymer and one of the blocks. When the incompatibility is weak, the microphase-separated stripe domains are perpendicular to an interface between the copolymer-rich and the homopolymer-rich phases whereas when it is strong the domains tend to be parallel to the interface. An analytical theory calculating the interfacial energy is presented to understand this transition.

PACS number(s): 36.20.−r, 64.60.Cn

I. INTRODUCTION

Microphase separation in block copolymers has been studied both experimentally and theoretically for more than two decades [1]. Because of the connectivity of mutually incompatible monomer blocks, the phase separation causes spatially periodic equilibrium structures such as lamellar, cylindrical hexogonal, spherical bcc, and regular three-dimensional bicontinuous structures. These ordered states arise by changing the block ratio. Since the spatial period is typically of the order of several hundred angstrom, we call the ordered state a mesophase.

The prediction of a possible mesophase for given parameters such as the block ratio and temperature is one of the most important problems. Recently, some of the ordered states have been confirmed theoretically by comparing the equilibrium free energy for each structure [2–17]. Another fundamental problem is to study kinetics of the microphase separation. Compared to the equilibrium structures, however, there are only a few works on the kinetics [18–20].

As was mentioned above, the block ratio is a key parameter for the equilibrium morphological transitions. In order to change the block ratio effectively, experimentalists often add a small amount of homopolymers as a selective solvent [21]. If one adds A homopolymer chains in a A-B diblock copolymer melt, these are resolved in the A-rich domains in the microphase-separated state. Thus one can increase effectively the ratio of the block length of A monomers to that of B monomers.

If one increases further the volume fraction of the added homopolymer, a qualitatively different behavior appears. Since the B block and A homopolymer are incompatible, one may expect a macrophase separation between the diblock copolymer and the homopolymer. This problem was addressed theoretically for general copolymer-homopolymer mixtures by Hong and Noolandi [4]. They predicted a macrophase separation at low temperatures, which is followed by a microphase separation in the copolymer-rich domains. However, they have not studied the dynamics of phase separation.

Quite recently, Koizumi, Hasegawa, and Hashimoto [22] carried out an experimental study of the phase separation of binary mixtures of polystyrene-*block*-polyisoprene (SI) and homopolystyrene (HS). In the case of a low volume fraction of SI, they observed the macrophase separation during the solvent evaporation process, which is subsequently followed by the microphase separation. When a lamellar structure is formed in the copolymer-rich domains, an onionlike pattern dispersed in a continuous matrix of HS is observed by transmission electron microscopy. In the case of the mixture with a cylinder-forming block copolymer, the macrodomains take a lenslike shape, in which cylindrical microdomains are packed hexagonally.

In this paper, we study the dynamics and morphology of phase separation in diblock copolymer-homopolymer mixtures. Each copolymer chain is composed of A and B monomers with a short-range repulsive interaction between them. The interaction between the homopolymer with C monomers and the B monomers in the copolymer is also assumed to be repulsive. We will show that a macrophase separation triggers a microphase separation for suitable volume fractions and chain lengths and hence curious domain patterns appear. The kinetics of this double phase separation and domain morphology will be investigated in detail.

We here introduce a simple dynamical model in terms of the local volume fractions of each monomer, which is an extension of the static theory of microphase separation [6]. Some of the investigators [2,9,11] have developed, for the equilibrium problem, a formulation based on a

more microscopic picture in terms of chain conformation. However, such an approach is not very useful for the domain growth problem in the course of phase separation. An analytical treatment of the chain motion in randomly interconnected domains seems formidable and computer simulations of chain dynamics are difficult to perform for a large system where sufficiently many domains must be contained. We have shown in a previous study [23] that the coarse-grained method in terms of the local volume fractions has predicted anomalous rheological properties of microphase-separated structures.

We shall carry out computer simulations of the model system in two dimensions by means of a cell dynamical method [24]. Computer simulations indeed reveal a double phase separation. That is, a macrophase separation between the copolymers and the homopolymers takes place first, and then a microphase separation proceeds in the copolymer-rich phase. Depending on the block ratio of the copolymer chains, lamellar and hexagonal domains appear. One of the remarkable results obtained by simulations is that there is a morphological transition in the lamellar structure. When the repulsive interaction between the homopolymers and the B blocks is weak, the lamellar domains are perpendicular to the interfaces that separate the copolymer- and homopolymer-rich domains, while when the interaction is sufficiently strong the striped domains are parallel to the interfaces.

In order to investigate the kinetics of the above double phase separation, we evaluate the scattering function in the course of the domain growth. It is shown that the domain morphology and the kinetics are mutually correlated. That is, the domain growth for the perpendicular morphology is not much different from that in an ordinary spinodal decomposition. However, in the case of the parallel morphology, growth of the macrophase-separated domains becomes extremely slow.

Because both the macrophase and microphase separations occur in the present system, the domain patterns are complicated. We use the following terminology in order to avoid confusion. By a macrodomain, we mean a domain caused by the macrophase separation. On the other hand, a microdomain is a domain of a lamellar or hexagonal structure due to the microphase separation. We also often use the word "macrointerface" indicating a boundary separating macrodomains of copolymer-rich and homopolymer-rich phases.

In the next section, we describe our model equations. The results of computer simulations are presented in Sec. III. In Sec. IV, we develop a theory for the morphological change from the parallel to the perpendicular structures of lamellar domains. Calculation of the interfacial energy of each structure shows a clear morphological transition by changing the interaction strength. We give discussions and concluding remarks in Sec. V.

II. DYNAMICAL MODEL

We consider a system with A-B diblock copolymer and C homopolymer having the polymerization indices N_A, N_B, and N_C. The block ratio f is defined by $f=N_A/(N_A+N_B)$. The local volume fractions of these monomers are denoted, respectively, by ϕ_a, ϕ_b, and ϕ_c. Under the incompressibility condition, two of these are independent. It is convenient to take $\phi=\phi_a-\phi_b$ and $\psi=\phi_a+\phi_b$ as the independent variables. That is, the variable ψ is useful to describe segregation of the copolymer and the homopolymer while ϕ plays a role of an order parameter in a microphase separation as in the previous theories [3,6]. The model free energy for copolymer-homopolymer mixtures in terms of ψ and ϕ consists of short-range and long-range parts:

$$F\{\psi,\phi\}=F_S\{\psi,\phi\}+F_L\{\psi,\phi\} \ . \tag{2.1}$$

The short-range part F_S is the usual Ginzburg-Landau-type free energy and is given by

$$F_S\{\psi,\phi\}=\int dr\left[\frac{c_1}{2}(\nabla\psi)^2+\frac{c_2}{2}(\nabla\phi)^2+W(\psi,\phi)\right] , \tag{2.2}$$

where c_1 and c_2 are positive constants. The local interaction W is generally difficult to evaluate from first principles. One of the simplifications is to employ the Flory-Huggins approximation as was done in Ref. [25] where the A-B copolymer is regarded as an A-B polymer blend. However, we here take a phenomenological approach and assume the form of W as

$$W(\eta,\phi)=g_1(\eta)+g_2(\phi)+b_1\eta\phi-\tfrac{1}{2}b_2\eta\phi^2-\tfrac{1}{2}b_3\eta^2\phi \ , \tag{2.3}$$

where b_1 and b_2 are positive constants. The other constant b_3 vanishes for $f=\frac{1}{2}$ and put as $b_3=b_0(1/N_A-1/N_B)$ with b_0 a positive constant. We have introduced a new variable η as $\eta=\psi-\psi_c$ where ψ_c is the volume fraction at the critical point of the macrophase separation. The functions $g_1(\eta)$ and $g_2(\phi)$ are assumed to be an even function with respect to the argument. Below the macrophase-separation temperature, $g_1(\eta)$ exhibits a double-well potential. On the other hand, $g_2(\phi)$ is not necessarily double well in the macrophase-separated state.

The physical meanings of the remaining three terms in (2.3) are clear. The term with the factor b_1 arises from the short-range interaction between the monomers. Let us put the interaction strength between i and j monomers as u_{ij} $(i,j=A,B,C)$ so that the energy arising from the short-range interaction is written as

$$\frac{1}{2}\sum_{i,j}u_{ij}\int dr\phi_i\phi_j \ . \tag{2.4a}$$

The constant b_1 is given in terms of u_{ij} by

$$b_1=\tfrac{1}{4}(u_{AA}-u_{BB})-\tfrac{1}{2}(u_{AC}-u_{BC}) \ . \tag{2.4b}$$

Thus when the repulsive interaction between the B block and C homopolymer is sufficiently strong compared to other pairs, the constant b_1 is positive.

The term with the coefficient b_2 violates the symmetry of the free energy under the transformation $\eta\rightarrow-\eta$ and $\phi\rightarrow-\phi$. This term is necessary in order to require that a microphase separation should occur only in the

copolymer-rich phase. In fact, the b_2 term implies that a large absolute value of ϕ is energetically favorable in the region $\eta > 0$.

In order for the last term to be invariant under the transformation $\eta \to -\eta$ and $\phi \to -\phi$, the constant b_3 must change sign under the interchange between A and B. The expression for b_3 given just below (2.3) indeed satisfies this condition.

Finally, we should mention that the terms linear in η and ϕ have been ignored in (2.3) because they are redundant to the dynamics. Thus (2.3) is the minimal model for the short-range part of the free energy of the copolymer-homopolymer mixtures.

We have verified that the Flory-Huggins-type approximation mentioned above and an expansion in powers of η indeed give us a local part like (2.3). It is noted that the free energy (2.3) has a similarity to those studied in eutectic growth [26] and microemulsions [27].

One of the characteristic features of the copolymer systems is that there is a Coulomb-type long-range repulsive interaction in the free-energy functional [6]. This long-range interaction originates from the reduction of conformation entropy of each polymer chain due to the chain connectivity at a junction point. It is emphasized that coexistence of a repulsive long-range interaction and the attractive short-range one as the second term in (2.2) is a fundamental mechanism for a periodic structure in equilibrium [28,29].

In the present case, the long-range part is given by

$$F_L\{\psi,\phi\} = \int dr \int dr' G(\mathbf{r},\mathbf{r}') \times \left[\frac{\alpha}{2}\delta\phi(\mathbf{r})\delta\phi(\mathbf{r}') + \beta\delta\phi(\mathbf{r})\delta\psi(\mathbf{r}') + \frac{\gamma}{2}\delta\psi(\mathbf{r})\delta\psi(\mathbf{r}') \right] , \tag{2.5}$$

where $G(\mathbf{r},\mathbf{r}')$ is defined through the relation $-\nabla^2 G(\mathbf{r},\mathbf{r}') = \delta(\mathbf{r}-\mathbf{r}')$ and $\delta\phi(\mathbf{r}) = \phi(\mathbf{r}) - \bar{\phi}$ with $\bar{\phi}$ the spatial average of ϕ. The constants α, β, and γ are given, respectively, by

$$\alpha = a\left[\frac{1}{N_A} + \frac{1}{N_B}\right]^2 , \tag{2.6a}$$

$$\beta = a\left[\frac{1}{N_A^2} - \frac{1}{N_B^2}\right] , \tag{2.6b}$$

$$\gamma = a\left[\frac{1}{N_A} - \frac{1}{N_B}\right]^2 , \tag{2.6c}$$

where a is a positive constant. These formulas can be derived from Eqs. (A.20) and (D.3) in Ref. [6].

Note the relation $\beta^2 = \alpha\gamma$ so that there must be a zero eigenvalue for the matrix M with the elements $M_{11} = \alpha$, $M_{12} = M_{21} = \beta$, and $M_{22} = \gamma$. In fact, by the linear transformation

$$\phi' = \frac{1}{\sqrt{\beta^2+\gamma^2}}(\gamma\psi + \beta\phi) , \tag{2.7a}$$

$$\psi' = \frac{1}{\sqrt{\beta^2+\gamma^2}}(\gamma\psi - \beta\phi) , \tag{2.7a}$$

the matrix M is diagonalized and the free energy F_L simply becomes

$$F_L = \tfrac{1}{2}(\alpha+\gamma)\int dr \int dr' G(\mathbf{r},\mathbf{r}')\phi'(\mathbf{r})\phi'(\mathbf{r}') . \tag{2.8}$$

It is noted from (2.6) and (2.7) that the spatial average of ϕ' is identically zero.

The equilibrium property is readily calculated from (2.2) and (2.8). For instance, the phase diagram for the spinodal lines of the macrophase and microphase separations is found to be essentially the same as that in Fig. 8(b) in Ref. [22].

Now we construct a dynamical model. First of all, we omit any hydrodynamic effects. The hydrodynamic interaction between polymer chains may not be entirely ignored in the kinetics of phase separation even in copolymer-homopolymer melts. However, simulations including the hydrodynamic interaction is time consuming. Furthermore, we expect that the morphological change of ordered domains found in the simulations described in the next section is not altered qualitatively by the hydrodynamic effects. Second, we do not consider thermal fluctuations since the domain growth in the length scale of several tens of nanometers is not much influenced by thermal fluctuations except for the very early stage.

Thus the phase separation of copolymer-homopolymer mixtures is modeled by the following coupled set of equations in terms of ϕ and ψ:

$$\frac{\partial\psi}{\partial t} = L_1\nabla^2\frac{\delta F}{\delta\psi} , \tag{2.9a}$$

$$\frac{\partial\phi}{\partial t} = L_2\nabla^2\frac{\delta F}{\delta\phi} , \tag{2.9b}$$

where the transport coefficients L_1 and L_2 are positive. The relative magnitude of these coefficients are not known experimentally. Here we assume, for simplicity, that these two are comparable. Since a polymer chain is an extended object, a nonlocal effect in the length scale of the radius of gyration appears generally in the transport coefficients [30,31]. However, we have neglected it as well as the possible dependence of L_1 and L_2 on ϕ and ψ.

III. COMPUTER SIMULATIONS

We have carried out computer simulations of Eqs. (2.9) by a cell dynamical system approach [24]. In two dimensions, the space is divided into 128×128 square cells with periodic boundary conditions. The size of a cell is put to be unity. The form of the local interactions $g_i(x)$ ($i = 1$ and 2) is chosen as $dg_i(x)/dx = -A_i \tanh x + x$ with the coefficient $A_1 = 1.3$ and $A_2 = 1.1$. Thus the macrophase separation takes place first. As the value of ϕ increases, the microphase separation starts because of the interaction term $\eta\phi^2$ in (2.3). The initial values of ϕ and η at each cell are assigned randomly around their spatial averages. The Onsager coefficients L_1 and L_2 are assumed to be the same; $L_1 = L_2 = 1$.

Because ψ is the volume fraction of the copolymer, its absolute value must be smaller than unity. In the above choice of g_i, however, we have removed this condition supposing that ψ and ϕ are suitably rescaled.

A. Lamellar microdomains

First, we consider the case of $f=\frac{1}{2}$ where a lamellar structure is expected to appear in a microphase-separated phase. The constants b_3, β, and γ in (2.3) and (2.5) vanish identically.

Figure 1 displays the domain growth obtained for $\bar{\phi}=\bar{\eta}=0$, $c_1=c_2=0.5$, $\alpha=0.02$, $b_1=0.07$, and $b_2=0.2$ at $t=1000$, 4000, 16 000, and 64 000 from top to bottom. A copolymer-rich domain for $\eta>0$ is drawn by gray color whereas a homopolymer-rich domain for $\eta<0$ is indicated by white color. In this figure as well as in Figs. 2–4 below, the regions where ϕ is larger than 0.15 are shown by black color. The spatial variation of ϕ and η along the line $y=64$ is shown in the figures on the right-hand side. At an early stage $t=1000$, interconnected domains of gray and black colors appear. This is the macrophase separation between the copolymer-rich and the homopolymer-rich phases. Since there are fairly large amount of A blocks in the homopolymer-rich domains, those are drawn not by white but by black color. Actually one can see that there are more A blocks in the homopolymer-rich domains and more B blocks in the copolymer-rich ones. However, this does not mean a microphase separation since the magnitude of their spatial variation is weak. What happens is that the wavelength of the variation of ϕ is forced to be comparable to the characteristic domain width of macrodomains. This will be clearer in Fig. 7(c) below.

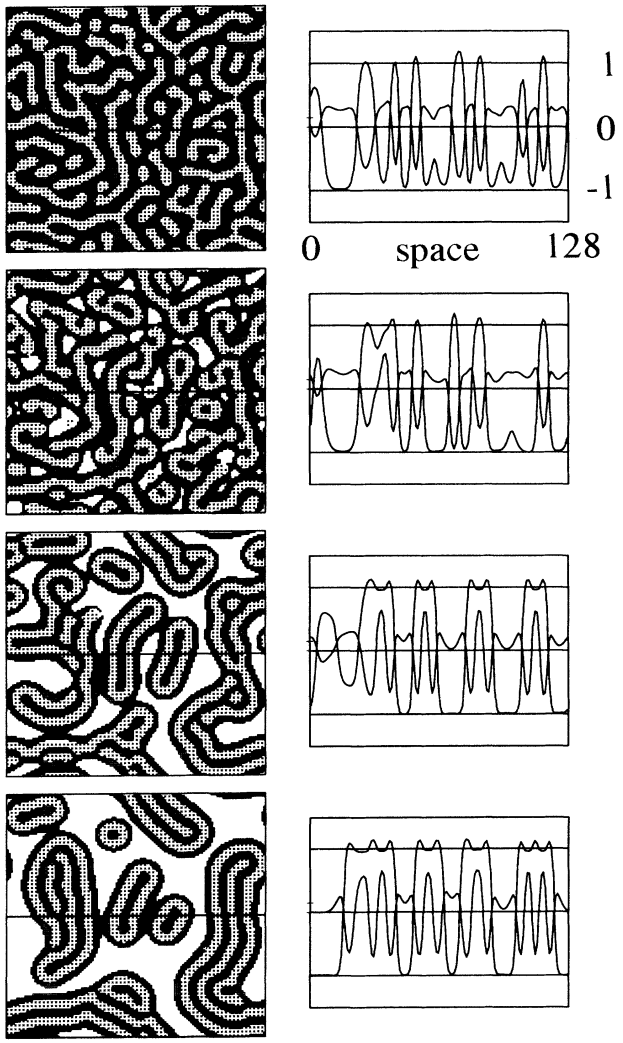

FIG. 1. Domain pattern for $\bar{\phi}=\bar{\eta}=0$ and $b_1=0.07$ at $t=1000$, 4000, 16 000, and 64 000 from top to bottom. The system size is 128×128. The white color indicates a homopolymer-rich domain. The gray (black) color indicates a domain where ϕ is smaller (larger) than 0.15. The figures on the right-hand side display the profile of $\phi(x)$ and $\eta(x)$ along the line $y=64$. The scale of the axes is shown in the top figure. The line with the larger amplitude indicates $\eta(x)$ whereas the line with smaller amplitude is $\phi(x)$.

The microphase separation starts only at about $t=4000$ after copolymer-rich domains become sufficiently large. It is noted that as the phase separation proceeds, the random bicontinuous domains change to disconnected copolymer-rich domains. This arises, for $b_1=0.07$, from the strong violation of the symmetry of the local part W in (2.3) under the interchange $\eta\rightarrow-\eta$.

It should be noted that in most parts of the macrodomains, the lamellar domains tend to be parallel to the macrophase interfaces and that each copolymer-rich domain is surrounded by a thin layer of the A blocks. The domain patterns in Fig. 1 are qualitatively quite similar to those observed experimentally by a transmission microscope [32].

This should be compared with the pattern evolution in Fig. 2 where $b_1=0.03$ and other constants and time steps are the same as those in Fig. 1. There are white domains even at $t=1000$, indicating that the A blocks are not much dissolved in the homopolymer-rich domains because of the weakness of the interaction b_1. As the microphase separation proceeds, the stripe domains emerge perpendicularly to the macrophase interfaces. Thus there is a clear morphological transition by changing the interaction parameter b_1. We have examined the transition in detail by changing the value of b_1 and found that the morphological change occurs at about $b_1=0.04$. In Fig. 2, the asymmetry of the pattern between the copolymer-rich and homopolymer-rich domains at the later stage is weak compared to that in Fig. 1.

Figure 3 is the pattern evolution for $\bar{\phi}=0$, $\bar{\eta}=-0.2$, and $b_1=0.05$ where disk-shaped domains grow. A concentric pattern due to the microphase separation emerges in each domain. Since the average size of domains is rather small and is comparable to the period of the microphase-separated structure, there are no onion-ring-like domains with many layers. As will be shown in Fig. 8, once concentric domains are formed, the kinetics of the macrophase separation becomes extremely slow.

If we decrease the value of b_1 slightly as $b_1=0.03$, we have a different morphology as shown in Fig. 4. That is,

at an early stage of the macrophase separation where the domains are small, the pattern is concentric. However, as the macrophase-separated domains become large, the microphase-separated domains tend to be perpendicular to the macrophase interface. This is the same property as in Fig. 2. It is also evident that there is a tendency such that the lamellar domains are parallel to the short principal axis of an elliptic macrodomain. One can also see from Figs. 3 and 4 that the growth kinetics is slower in Fig. 3.

B. Hexagonal microdomains

When the block ratio f is away from $\frac{1}{2}$, a lamellar structure becomes unstable and a hexagonal structure of disconnected domains is formed. Here we study the double phase separation for $\bar{\phi}=-0.2$ which roughly corresponds to $f=0.4$. In this case, the coefficients of all the terms in (2.2), (2.3), and (2.5) are nonvanishing. In the simulations, we fix these parameters as $b_2=0.2$, $b_3=0.01$, $\alpha=0.02$, $\beta=0.002$, and $\gamma=0.002$ and the spatial average $\bar{\eta}=0$.

Figures 5(a) and 5(b) display the domain patterns at $t=64\,000$ for $b_1=0.05$ and 0, respectively. A white area is the area where η is negative. The region where ϕ is positive is drawn in black. (Note that this is different from in Figs. 1–4.) The copolymer-rich domains tend to be rounded in Fig. 5(a) while the macrodomains in Fig. 5(b) are mutually interconnected. In Fig. 5(a) there is a thin layer of the A blocks just outside the copolymer-rich domains. We have verified numerically that the conservation of ϕ and η is satisfied in simulations. The hexagonal structures themselves are not much different from each other in these figures.

C. Scattering functions

In order to analyze the kinetics of the domain growth, we have made the Fourier transform of $\phi(\mathbf{r},t)$ and $\eta(\mathbf{r},t)$ at each time step and calculated the time evolution of the scattering intensities:

$$S_{\mathbf{k}}(t)=\langle \phi_{\mathbf{k}}\phi_{-\mathbf{k}}\rangle \tag{3.1a}$$

and

$$I_{\mathbf{k}}(t)=\langle \eta_{\mathbf{k}}\eta_{-\mathbf{k}}\rangle\ , \tag{3.1b}$$

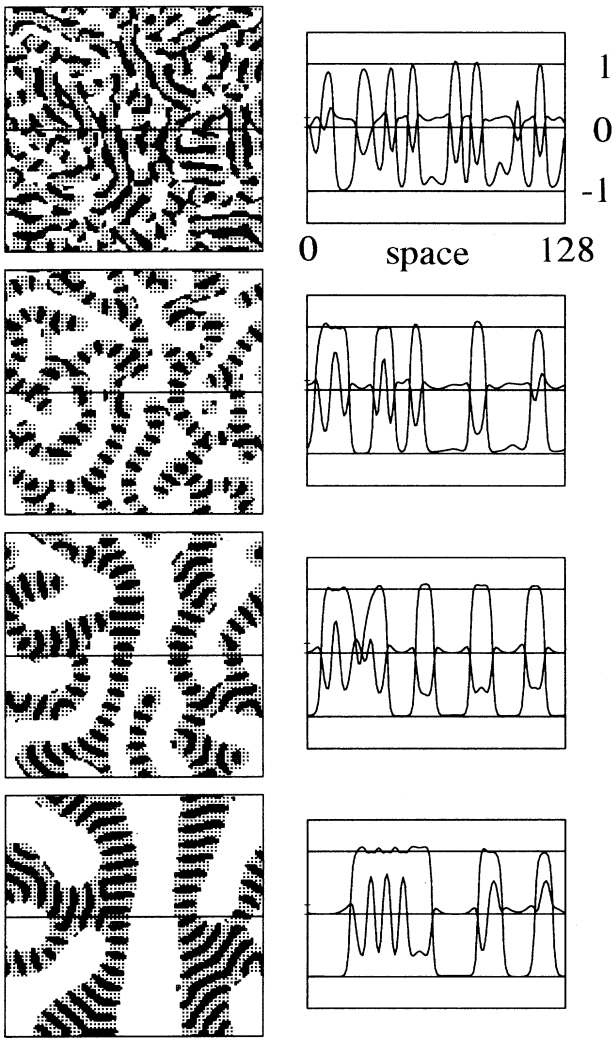

FIG. 2. Domain pattern for $\bar{\phi}=\bar{\eta}=0$ and $b_1=0.03$ at $t=1000$, 4000, 16 000, and 64 000 from top to bottom. Other details are the same as in Fig. 1.

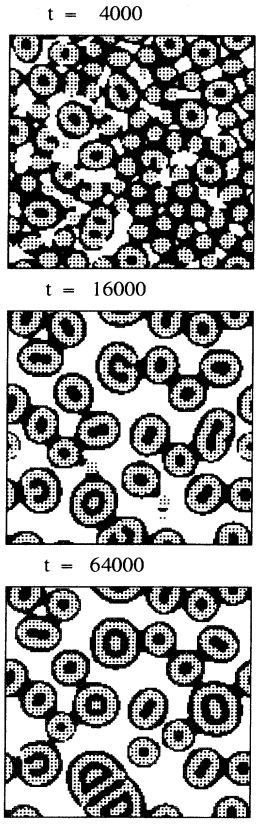

FIG. 3. Domain pattern for $\bar{\phi}=0$, $\bar{\eta}=-0.2$, and $b_1=0.05$ at $t=4000$, 16 000, and 64 000 from top to bottom. Other details are the same as in Fig. 1.

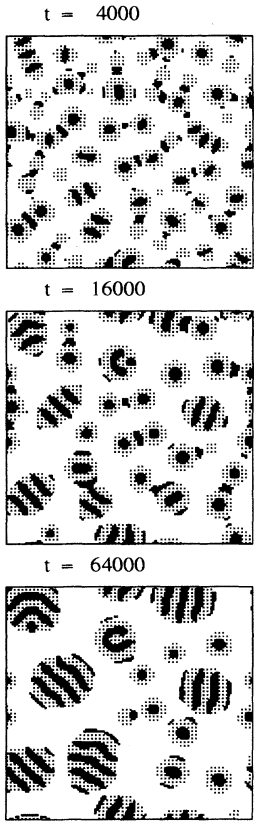

FIG. 4. Domain pattern for $\bar{\phi}=0$, $\bar{\eta}=-0.2$, and $b_1=0.03$ at $t=4000$, 16 000, and 64 000 from top to bottom. Other details are the same as in Fig. 1.

where the average $\langle \cdots \rangle$ is taken over the initial randomness. The scattering intensities are averaged over 10 independent runs.

Here we restrict ourselves to the case $f=\frac{1}{2}$. A typical example is shown in Fig. 6 for $\bar{\phi}=\bar{\eta}=b_1=0$. In this case, the microdomains take a perpendicular morphology. The left peaks are the intensity $I_{\mathbf{k}}(t)$ at $t=1000$, 2000, 4000, 8000, 16 000, and 32 000 from low to high peaks while the right ones show $S_{\mathbf{k}}(t)$ in the same manner. Note that we have different scales for $S_{\mathbf{k}}(t)$ and $I_{\mathbf{k}}(t)$. Actually $S_{\mathbf{k}}(t)$ is magnified by the factor of 25 compared with $I_{\mathbf{k}}(t)$. The time evolution of $I_{\mathbf{k}}(t)$ is qualitatively the same as that of an ordinary spinodal decomposition in polymer blends. The peak position k_M and the peak height I_M of $I_{\mathbf{k}}$ depend on time approximately as

$$k_M=t^{-a} \tag{3.2a}$$

and

$$I_M=t^{b} \tag{3.2b}$$

with $a=0.35$ and $b=0.64$. [The exponent a should not be confused with the constant a appeared in (2.6).] The exponents a and b are quite close to $\frac{1}{3}$ and $\frac{2}{3}$, respectively, which are expected in the late stage of ordinary spinodal decomposition. The peak position of the other intensity $S_{\mathbf{k}}(t)$ is almost time independent. This is expected for small values of b_1 since the merging microstructure is spatially periodic and the wave number of the initial unstable mode is not much different from that of the final structure in the weak segregation regime. The peak height S_M does not obey a power law but it grows slower at the later time.

The time dependence to the peak height and the peak position of the scattering functions is summarized in Figs. 7 and 8. These are a double logarithmic plot of the peak intensity versus time and the peak position versus time. Figure 7 compares the time evolution of the perpendicular and the parallel morphologies, respectively, for $b_1=0$ and 0.08. The average volume fractions are $\bar{\phi}=\bar{\eta}=0$. The exponent b of $I_{\mathbf{k}}$ for $b_1=0$ is estimated from the straight line in Fig. 7(a) and is given approximately by $b=0.64$ as mentioned above, while that for $b_1=0.08$ in Fig. 7(c) is smaller, i.e., $b=0.48$. The time dependence of $S_{\mathbf{k}}$ for $b_1=0$ is slower than a power law and is almost constant for $b_1=0.08$.

The exponent a for $I_{\mathbf{k}}$ is approximately equal to 0.35

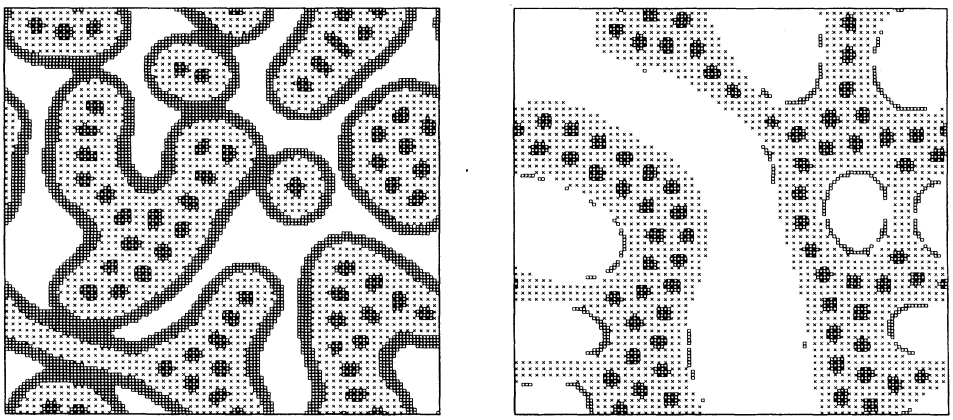

FIG. 5. Domain pattern at $t=64\,000$ for $\bar{\phi}=-0.2$, $\bar{\eta}=0$ and (a) for $b_1=0.05$ and (b) for $b_1=0$. A homopolymer-rich domain is indicated by while color. The microphase-separated domains are shown by black color for $\phi>0$ and gray color for $\phi<0$. Other details are the same as in Fig. 1.

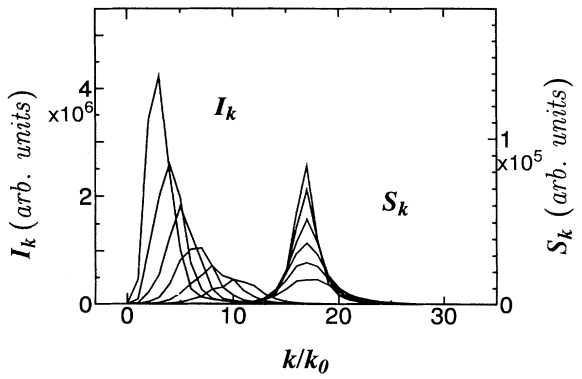

FIG. 6. Time evolution of the scattering functions I_k (left curves) and S_k (right curves) as a function of the wave number for $\bar{\phi}=\bar{\eta}=0$ and $b_1=0$. The scaled wave number k_0 is defined by $k_0=\pi/64$. The scale of the vertical axis in this figure and Figs. 7 and 8 below is in arbitrary units.

for $b_1=0$ and to 0.36 for $b_1=0.08$. It is noted that the peak wave number of S_k for $b_1=0.08$ slightly increases with time. In the early stage of macrophase separation, the spatial variation of ϕ is adjusted by the average size of the macrodomains as was mentioned in Sec. III A. This is the reason that the peak wave number of I_k and S_k is almost the same value initially as can be seen in Fig. 7(d). As the macrodomains grow, another microdomain can merge in a macrodomain so that the characteristic wave number for microdomains increases. This is an important property of domain growth in the parallel morphology.

Figure 8 shows the kinetics of disconnected macrodomains for $\bar{\phi}=0$ and $\bar{\eta}=-0.2$. We compare again two morphologies for $b_1=0$ and 0.05. The exponents a and b for $b_1=0$ in Figs. 8(a) and 8(b) are approximately given by $a=0.27$ and $b=0.53$. On the other hand, the peak height of I_k in Fig. 8(c) for onion-ring-like domains, $b_1=0.05$, ceases apparently to grow at a later time. A similar behavior can also be seen in the time evolution of the peak position as in Fig. 8(d). This is another characteristic feature of the parallel domain morphology. Because of the finite-size effect, however, it is difficult to confirm whether the domains presumably stop to grow or not.

IV. INTERFACIAL ENERGY

In order to understand the morphological transition observed by computer simulations in the preceding section, here we calculate the interfacial energy of a macrophase-separated domain boundary. As depicted in Fig. 9, we consider two kinds of lamellar structures for $f=\frac{1}{2}$. Figure 9(a) displays a domain configuration where

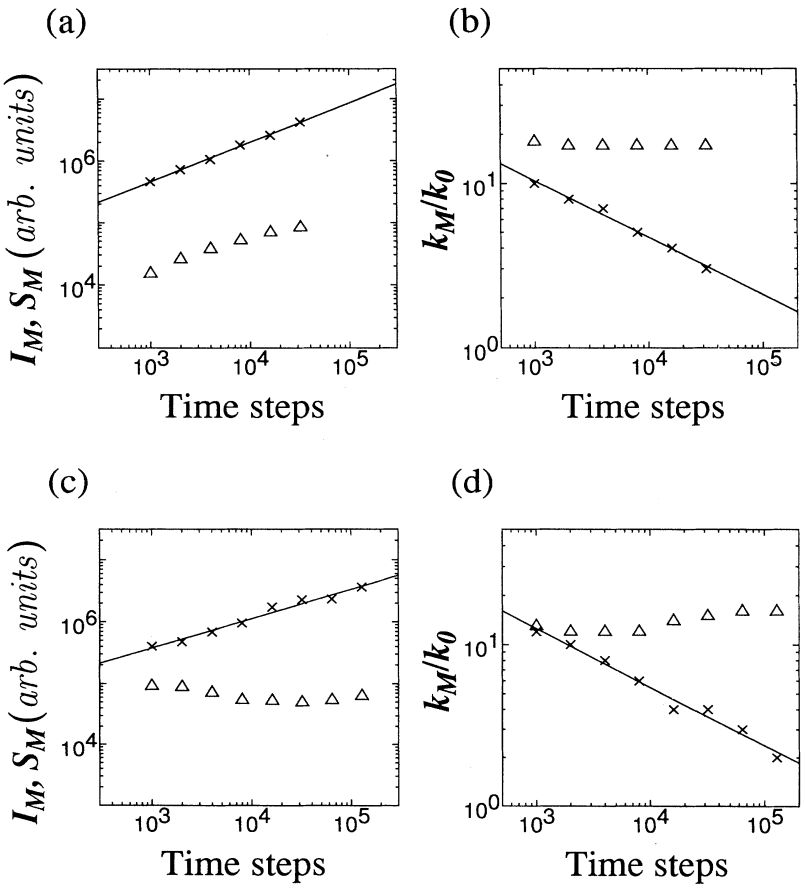

FIG. 7. Time evolution of the peak intensity and the peak height for $\bar{\phi}=\bar{\eta}=0$. The crosses indicate the value associated with I_k while the triangles indicate the value of S_k. (a) Intensity for $b_1=0$, (b) peak position for $b_1=0$, (c) intensity for $b_1=0.08$, and (d) peak position for $b_1=0.08$.

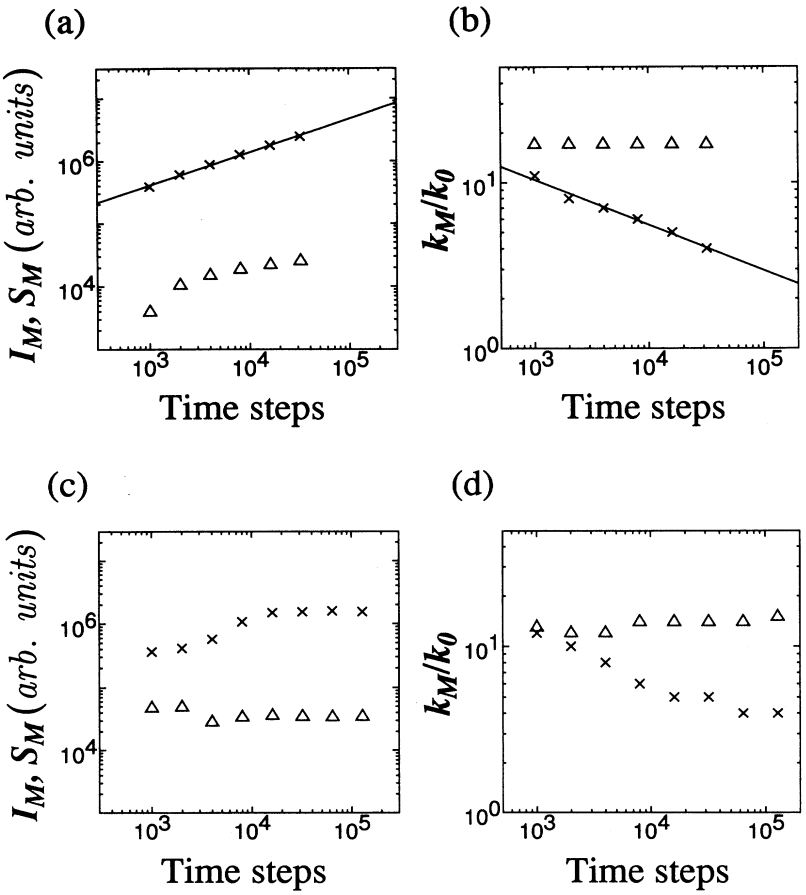

FIG. 8. Time evolution of the peak intensity and the peak height for $\bar{\phi}=0$ and $\bar{\eta}=-0.2$. The meaning of the symbols is the same as that in Fig. 7. (a) Intensity for $b_1=0$, (b) peak position for $b_1=0$, (c) intensity for $b_1=0.05$, and (d) peak position for $b_1=0.05$.

a homopolymer-rich phase is on the left half plane $x<0$, while on the right half plane, there are microphase-separated stripe domains that are perpendicular to the interface located at $x=0$. On the other hand, the lamellar domains are parallel to the interface in Fig. 9(b). We shall calculate the free energy of each domain structure by means of a variational method. Without loss of generality, we restrict ourselves to two dimensions. Hereafter we call the domain pattern in Fig. 9(a) case I and that in Fig. 9(b) case II.

We assume that the interface width is much smaller than the spatial period of the lamellar structure and that the microphase separation is in a weak segregation regime. This is in accord with the present computer simulations. Because of the existence of a macrophase boundary, the lamellar structure is generally expected to be deformed near the interface. However, we ignore this effect avoiding an unessential complication in the theoretical treatment.

When $f=\frac{1}{2}$, the free energy (2.1) turns out to be

$$F\{\eta,\phi\}=\int dr\left[\frac{c_1}{2}(\nabla\eta)^2+\frac{c_2}{2}(\nabla\phi)^2+g_1(\eta)+g_2(\phi)+b_1\eta\phi-\frac{1}{2}b_2\eta\phi^2\right]$$
$$+\frac{\alpha}{2}\int dr\int dr' G(\mathbf{r},\mathbf{r}')[\phi(\mathbf{r})-\bar{\phi}][\phi(\mathbf{r}')-\bar{\phi}]\ . \tag{4.1}$$

The spatial variation of ϕ in the weak segregation regime can be written as $\phi\propto\cos qx$. The wave number q is determined by the minimization of the nonlocal terms in (4.1), i.e., the second and the last terms. After the Fourier transform, those are given by

$$\int dq\left[\frac{c_2}{2}q^2+\frac{\alpha}{2}\frac{1}{q^2}\right]\phi_{\mathbf{q}}\phi_{-\mathbf{q}}\ . \tag{4.2}$$

This gives us the first growing wave number q_c at the transition point as $q_c^2=(\alpha/c_2)^{1/2}$. In the weak segregation, we may expand $1/q^2$ in the long-range interaction in powers of $q^2-q_c^2$ so that the free energy (4.1) becomes the Brazovskii form [3,33]

$$F\{\eta,\phi\}=\int dr\left[\frac{c_1}{2}(\nabla\eta)^2-\frac{\alpha}{q_c^4}(\nabla\phi)^2+\frac{\alpha}{2q_c^6}(\nabla^2\phi)^2\right.$$
$$\left.+\frac{3\alpha}{2q_c^2}\phi^2+(\text{other local parts})\right]\ , \tag{4.3}$$

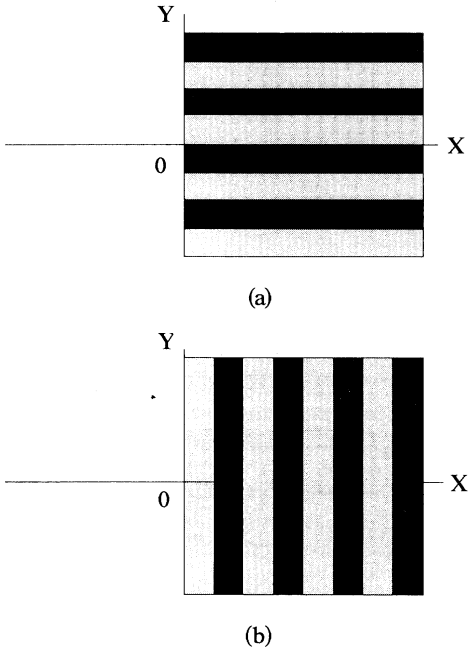

FIG. 9. Schematic representation of (a) perpendicular configuration and (b) parallel configuration. A macrointerface separating a homopolymer-rich phase ($x<0$) and copolymer-rich phase ($x>0$) is along the line $x=0$.

where we have ignored an additive constant.

Now we consider the domain structure of the case I. We put the nonuniform equilibrium solutions of η and ϕ as

$$\eta(x)=A\tanh kx\ , \tag{4.4}$$

$$\phi(x)=\frac{AB}{2}(1+\tanh kx)\sin q_c y\ , \tag{4.5}$$

where the constants A, B, and k should be determined by the minimization of (4.3). It will be shown below, however, that these precise values are unnecessary in comparison with the interfacial energy.

Substitution of (4.4) and (4.5) into (4.3) yields the equilibrium free energy for the domain configuration of case I. In this calculation, we employ an approximation such that all the higher harmonics of $\sin q_c y$ are neglected. This is allowed in a weak segregation limit. It is readily seen that each term in (4.3) causes two different contributions. One is the bulk free energy proportional to the system size. The other is linearly dependent on the interface length (area). We identify this with the interfacial energy. For instance, we obtain

$$\int dr(\nabla\phi)^2=\left[\frac{ABq_c}{2}\right]^2\frac{1}{k}L_xL_y+\left[\frac{ABk}{2}\right]^2\frac{1}{2k}C_{40}L_y-\left[\frac{ABq_c}{2}\right]^2\frac{1}{2k}C_{20}L_y\ , \tag{4.6}$$

where L_x (L_y) is the linear dimension of the x (y) direction of the system. The constant C_{mn} is defined by

$$C_{mn}=\int_{-\infty}^{\infty}dx\frac{\sinh^n x}{\cosh^m x}\ . \tag{4.7}$$

One of the important facts is that because of the factor $\sin q_c y$ in (4.5), the term linear in ϕ in (4.3) vanishes identically:

$$b_1\int dr\,\eta\phi=0\ . \tag{4.8}$$

Next we evaluate the equilibrium free energy for case II. The profile of η is the same as (4.4). The lamellar structure in Fig. 9(b) is expressed as

$$\phi(x)=\frac{AB}{2}(1+\tanh kx)\cos[q_c(x-x_0)]\ , \tag{4.9}$$

where we have introduced the phase factor x_0, which will play an essential role in the interfacial energy and will be determined by the free-energy minimization.

As in case I, we substitute (4.4) and (4.9) into (4.3) ignoring the higher harmonics of $\cos[q_c(x-x_0)]$. The contributions from each term in (4.3) are almost the same as those in case I. The difference appears only in the following two terms:

$$\int dr(\nabla^2\phi)^2=\left[\frac{ABq_c^2}{2}\right]^2\frac{1}{k}L_xL_y+L_y\left\{\left[\frac{ABk^2}{2}\right]^2\frac{2}{k}C_{62}+(ABkq_c)^2\frac{1}{2k}C_{40}-\left[\frac{ABq_c^2}{2}\right]^2\frac{1}{2k}C_{20}+(ABk^2)(ABq_c^2)\frac{1}{2k}C_{42}\right\}\ , \tag{4.10}$$

$$\int dr\,\eta\phi=L_y\frac{A^2B}{2}\frac{1}{q_c}C_{20}\sin q_c x_0\ . \tag{4.11}$$

In case I, the second term in curly brackets in (4.10) does not exist. (4.11) was identically zero in case I as mentioned above. When the macrophase separation is in strong segregation, i.e., $2\pi k/q_c\gg 1$ as we have assumed, the first term in curly brackets in (4.10), which is positive, is most dominant in the interfacial energy. From this fact together with (4.11), the interfacial energy is found to take a minimum value at $q_c x_0=-\pi/2$.

In this way, we obtain the difference of the interfacial energies $\sigma_{\rm I}$ and $\sigma_{\rm II}$ of cases I and II as

$$\sigma_{\rm II}-\sigma_{\rm I}=\frac{A^2B}{2}\frac{1}{q_c}\left[\frac{\alpha\beta}{2q_c^3}kC_{40}-b_1C_{20}\right]\ . \tag{4.12}$$

This implies that when the condition

$$b_1 > b_1^c = \frac{\alpha B}{2q_c^3} k \frac{C_{40}}{C_{20}} = \frac{1}{3} \frac{\alpha B}{q_c^3} k \tag{4.13}$$

is satisfied, the interfacial energy σ_{II} is lower than σ_I. We have used the facts that the $C_{20}=2$ and $C_{40}=\frac{4}{3}$. Thus if one increases the incompatibility strength b_1 defined by (2.4b), case II is energetically more favorable than case I. Thus the domains tend to align parallel to the macrophase interfaces.

Using the values $\alpha=0.02$, $B\approx 0.6$, $k\approx 0.3$ and $q_c\approx 0.45$ consistent with the simulations, the critical value b_1^c is estimated from (4.13) as $b_1^c\approx 0.01-0.02$. This is slightly smaller than but qualitatively in agreement with $b_1^c\approx 0.04$ obtained by simulations.

The reason as to why the theoretical value of b_1^c is smaller than that of simulations can be understood partly as follows: Lamellar domains start to grow in the center part of a copolymer-rich domain, which is randomly interconnected with the homopolymer-rich one. Since the system is isotropic and there is no preferable orientation of the lamellar structure, it is statistically rare that the microphase-separated stripe domains happen to be parallel to the macrointerfaces. As a result, the microdomains must touch the macrointerfaces as they grow. This occurs when the value of b_1 is not very large. Once this happens, the lamellar domains tend to align perpendicularly to the macrointerfaces to diminish the energy between A-rich and B-rich microdomains, i.e, the length of the stripe. Although this perpendicular configuration causes higher interfacial energy of the macrointerface for moderate values of b_1, the microdomains cannot reorient to a parallel configuration because it requires reconnection of the domains and causes extra energy. The above argument implies that the perpendicular morphology observed for $0.01<b_1<0.04$ is a metastable state.

As can be seen in Fig. 4 for small values of b_1, the lamellar domains are parallel to the smaller principal axis of an elliptic macrodomain. This is also understood by the interfacial argument. When b_1 is small, a domain configuration of the case I is energetically more favorable and hence the microdomains take the pattern as in Fig. 4 to enlarge the interfacial area of the case I. The situation is essentially the same as an equilibrium crystal shape determined by an anisotropic interfacial energy.

As was mentioned above, the phase factor is given by $q_c x_0=-\pi/2$. Substituting this into (4.9), we note that a small bump exists in the profile of ϕ just a copolymer-rich domain. This is consistent with spatial variation of ϕ shown in Fig. 1.

V. DISCUSSIONS

We have studied the phase separation in copolymer-homopolymer mixtures. Computer simulations of the model equations have indeed realized the double-phase separation. A morphological transition has been found by changing the interaction strength [34]. When b_1 is large, the microphase-separated lamellar domains are parallel to the macrointerfaces. When b_1 is smaller than about 0.04, the lamellar domains are perpendicular to the interfaces. We have confirmed theoretically that the difference of the interfacial energy for these two domain configurations is the origin of this transition [35].

The concentric domains obtained by simulations as in Fig. 3 have only a few lamellar layers. In principle, it is possible to realize a concentric domain having more layers by delaying the microphase separation, i.e., by changing the ratio A_1/A_2 introduced in the beginning of Sec. III. However, there is technical difficulty that the anisotropy due to the infinite cell size appears by changing these parameters so that we have not attempted to produce multilayer domains in the simulations starting from the disordered state.

We emphasize that the long-range interaction in (4.1) plays a decisive role of the morphological transition. If one considered only the local interaction given by the b_1 term in (4.1), one could not understand the existence of the perpendicular morphology. It should be noted, however, by an electrostatic analogy that the parallel morphology gives a larger contribution to the interfacial energy. This is indeed the case in (4.12), which indicates a competition between the b_1 term and the $(\nabla^2\phi)^2$ term which arises from the long-range interaction.

Kinetics of phase separation is also found to be affected by the growing domain morphology. The growth behavior of the perpendicular configuration is essentially the same as that of spinodal decomposition in polymer blends. On the other hand, the macrodomain growth especially for the block ratio $f=0.5$ and the volume fraction $\eta=-0.2$ is quite slow once the concentric microdomains are formed in the copolymer-rich macrodomains. It is a remaining problem to develop a theory for this slow kinetics, e.g., by means of an interfacial approach. However, in the picture of polymer chains, the anomalous growth can be understood as follows. Note from Fig. 1 that there are B blocks just inside a copolymer-rich domain. Since A blocks are compatible with C homopolymers in the matrix, they tend to accumulate just outside the macrointerface and form a small bump in the concentration profile. Thus a bilayer of A and B blocks is constituted along the macrointerface. This makes the interfacial energy low and furthermore inhibits the diffusion of the homopolymer chains across the interface of that coarsening of the macrodomains is suppressed. It is noted that this slow growth is similar somehow to that found in polymer blends with added copolymers as a surfactant [25].

We have considered a mixture of A-B diblock copolymers and C homopolymers. In this case, one may change the parameter b_1 without altering the macro- and the micro-phase-separation temperatures substantially if one chooses appropriately the interaction parameters u_{ij} in Eq. (2.4a). In the case of A-B copolymers and A homopolymers as in the experiments [22], varying b_1 would cause a shift of the transition temperatures and hence affect the degree of phase separation. Thus a mixture of

A-B diblock copolymers and *C* homopolymers will be more suitable to detect experimentally the morphological transition found in simulations.

Finally, we mention that phase separation of copolymer-copolymer mixtures is also studied by a generalization of the present model system, which will be published elsewhere in the near future.

ACKNOWLEDGMENTS

The authors are grateful to T. Hashimoto, S. Koizumi, and T. Kawakatsu for valuable discussions and informing us of their results prior to publications. One of the authors (A.I.) is supported by the Hayashi Memorial Foundation for Female Natural Scientists.

[1] F. S. Bates and G. H. Fredrickson, Annu. Rev. Phys. Chem. **41**, 525 (1990).
[2] E. Helfand and Z. R. Wasserman, Macromolecules **13**, 994 (1980), and the earlier references cited therein.
[3] L. Leibler, Macromolecules **13**, 1602 (1980).
[4] K. M. Hong and J. Noolandi, Macromolecules **16**, 1083 (1983).
[5] A. N. Semenov, Zh. Eksp. Teor. Fiz. **88**, 1242 (1985) [Sov. Phys. JETP **61**, 733 (1985)].
[6] T. Ohta and K. Kawasaki, Macromolecules **19**, 2621 (1986); **23**, 2413 (1990).
[7] G. Fredrickson and E. Helfand, J. Chem. Phys. **87**, 697 (1987).
[8] E. N. Thomas, D. M. Anderson, C. S. Henke, and D. Hoffman, Nature **334**, 589 (1988).
[9] K. Kawasaki and T. Kawakatsu, Macromolecules **23**, 4006 (1990).
[10] J. Melenkevitz and M. Muthukumar, Macromolecules **24**, 4199 (1991).
[11] K. R. Shull, Macromolecules **25**, 2122 (1992).
[12] R. J. Spontak and J. Zielinski, Macromolecules **25**, 663 (1992).
[13] H. Nakazawa and T. Ohta, Macromolecules **26**, 5503 (1993).
[14] M. W. Matsen and M. Schick, Phys. Rev. Lett. **72**, 2660 (1994); M. Schick and M. W. Masten, Macromolecules **27**, 7157 (1994).
[15] P. D. Olmsted and S. T. Milner, Phys. Rev. Lett. **72**, 936 (1994); **74**, 829 (1994).
[16] M. Muthukumar, Macromolecules **26**, 5259 (1993).
[17] A. N. Semenov, Macromolecules **27**, 3103 (1994).
[18] A. Chakrabarti, R. Toral, and J. D. Gunton, Phys. Rev. Lett. **63**, 2661 (1989).
[19] M. Laradji, M. Grant, and M. J. Zuckermann, Phys. Rev. B **41**, 4646 (1990); C. Roland and R. C. Desai, *ibid.* **42**, 6658 (1990).
[20] S. C. Glotzer and A. Coniglio, Phys. Rev. E **50**, 4241 (1994).
[21] See, for instance, M. Shibayama, T. Hashimoto, and H. Kawai, Macromolecules **16**, 16 (1983).
[22] S. Koizumi, H. Hasegawa, and T. Hashimoto, Macromolecules **27**, 6532 (1994).
[23] T. Ohta, Y. Enomoto, J. L. Harden, and M. Doi, Macromolecules **26**, 4928 (1993); M. Doi, J. L. Harden, and T. Ohta, *ibid.* **26**, 4935 (1993).
[24] Y. Oono and S. Puri, Phys. Rev. Lett. **58**, 836 (1987); S. Puri and Y. Oono, Phys. Rev. A **38**, 1542 (1988); M. Bahiana and Y. Oono, *ibid.* **41**, 6763 (1990); A. Shinozaki and Y. Oono, Phys. Rev. E **48**, 2622 (1993).
[25] T. Kawakatsu, Phys. Rev. E **50**, 2856 (1994).
[26] A. Karma, Phys. Rev. E **49**, 2245 (1994); K. R. Elder, F. Drolet, J. M. Kosterlitz, and M. Grant, Phys. Rev. Lett. **72**, 677 (1994).
[27] G. Gompper and M. Schick, Phys. Rev. E **49**, 1478 (1994).
[28] T. Ohta, A. Ito, and A. Tetsuka, Phys. Rev. A **42**, 3225 (1990).
[29] M. Seul and D. Andelman, Science **267**, 476 (1995).
[30] P. J. Pincus, J. Chem. Phys. **75**, 1996 (1981).
[31] K. Kawasaki and K. Sekimoto, Macromolecules **22**, 3063 (1989).
[32] T. Hashimoto (unpublished).
[33] S. A. Brazovskii, Zh. Eksp. Teor. Fiz. **68**, 175 (1975) [Sov. Phys. JETP **41**, 85 (1975)].
[34] We have carried out preliminary simulations in three dimensions and have confirmed that the morphological transition found here is also observed in three dimensions.
[35] A similar interfacial analysis has been done in a different context by Turner *et al.* [M. S. Turner, M. Rubinstein, and C. M. Marques, Macromolecules **27**, 4986 (1994)].

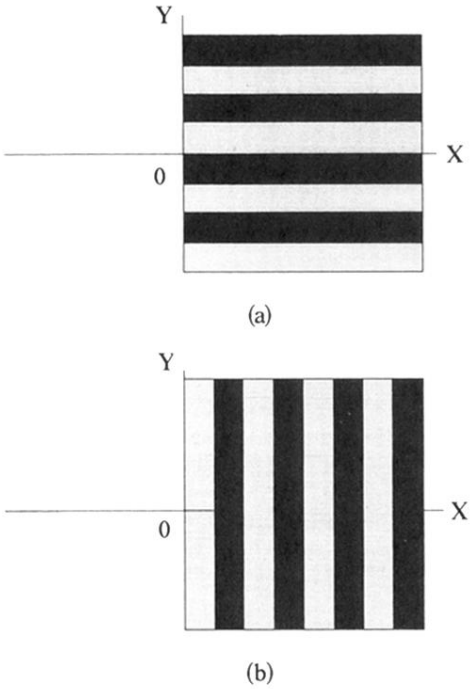

FIG. 9. Schematic representation of (a) perpendicular configuration and (b) parallel configuration. A macrointerface separating a homopolymer-rich phase ($x < 0$) and copolymer-rich phase ($x > 0$) is along the line $x = 0$.